HHS Public Access

Author manuscript

Bioelectrochemistry. Author manuscript; available in PMC 2019 June 01.

Published in final edited form as:

Bioelectrochemistry. 2018 June ; 121: 135–141. doi:10.1016/j.bioelechem.2018.01.013.

Electropermeabilization of cells by closely spaced paired nanosecond-range pulses

Iurii Semenov[a,1], **Maura Casciola**[a,1], **Bennet L. Ibey**[b], **Shu Xiao**[a,c], and **Andrei G. Pakhomov**[a,*]

[a]Frank Reidy Research Center for Bioelectrics, Old Dominion University, Norfolk, VA 23508, USA

[b]Radio Frequency Bioeffects Branch, Air Force Research Laboratories, Ft. Sam Houston, San Antonio, TX, USA

[c]Department of Electrical and Computer Engineering, Old Dominion University, Norfolk, VA 23508, USA

Abstract

Decreasing the time gap between two identical electric pulses is expected to render bioeffects similar to those of a single pulse of equivalent total duration. In this study, we show that it is not necessarily true, and that the effects vary for different permeabilization markers. We exposed individual CHO or NG108 cells to one 300-ns pulse (3.7–11.6 kV/cm), or a pair of such pulses (0.4–1000 μs interval), or to a single 600-ns pulse of the same amplitude. Electropermeabilization was evaluated (a) by the uptake of YO-PRO-1 (YP) dye; (b) by the amplitude of elicited Ca^{2+} transients, and (c) by the entry of Tl^{+} ions. For YP uptake, applying a 600-ns pulse or a pair of 300-ns pulses doubled the effect of a single 300-ns pulse; this additive effect did not depend on the time interval between pulses or the electric field, indicating that already permeabilized cells are as susceptible to electropermeabilization as naïve cells. In contrast, Ca^{2+} transients and Tl^{+} uptake increased in a supra-additive fashion when two pulses were delivered instead of one. Paired pulses at 3.7 kV/cm with minimal separation (0.4 and 1 μs) elicited 50–100% larger Ca^{2+} transients than either a single 600-ns pulse or paired pulses with longer separation (10–1000 μs). This paradoxically high efficiency of the closest spaced pulses was emphasized when Ca^{2+} transients were elicited in a Ca^{2+}-free solution (when the endoplasmic reticulum (ER) was the sole significant source of Ca^{2+}), but was eliminated by Ca^{2+} depletion from the ER and was not observed for Tl^{+} entry through the electropermeabilized membrane. We conclude that closely spaced paired pulses specifically target ER, by either permeabilizing it to a greater extent than a single double-duration pulse thus causing more Ca^{2+} leak, or by amplifying Ca^{2+}-induced Ca^{2+} release by an unknown mechanism.

*Corresponding author at: Frank Reidy Research Center for Bioelectrics, Old Dominion University, 4211 Monarch Way., Suite 300, Norfolk, VA 23508, USA. 2andrei@pakhomov.net, apakhomo@odu.edu (A.G. Pakhomov).

[1]Equal contribution.

Conflicts of interest

None.

Author contributions

A.G.P. and B.L.I. conceived and designed the study; I.S. and M.C. conducted the experiments and analyzed the data; M.C. performed the EF simulations for dosimetry calculations; S.X. designed and fabricated the pulser; all authors discussed and interpreted the data; A.G.P., M.C., I.S., and BLI wrote and edited the manuscript.

Keywords

Nanosecond pulses; Electroporation; Electropermeabilization; Nanopores; Membrane permeability

1. Introduction

Most electroporation treatments, from gene delivery to tissue ablation, require the delivery of multiple pulses to achieve the desired effect. However, even the first pulse(s) in a train disrupts the integrity of the cell membrane, reducing its electric resistance, and likely initiating adaptive biological responses. Therefore, an “already exposed” cell is different from a naïve cell, and its susceptibility to subsequent pulses will likely be different.

In the most widely accepted mechanism of electroporation, an externally applied electric field charges the cell membrane until it reaches a critical potential [1–3]. At this potential, pores (or other defects) form in the membrane, allowing membrane-impermeable solutes and ions to leak in and out of the cell. This leak current should prevent or slow down further build-up of the membrane potential if the external electric field is still applied, and hinder the membrane potential build-up from subsequent pulses. This way, the electroporation efficiency of pulses in a train should decrease with the sequential number of the pulse [4,5]. However, experimental measurements of the uptake of membrane-impermeable dyes (such as propidium or YP) often showed a simple linear dependence on the pulse number [6–9]. The membrane did not reseal between the pulses, as could be evidenced by dye uptake continuing much longer than the interpulse interval. The linear dependence of electroporation on the pulse number was interpreted as opening of a certain constant number of pores by each pulse in the train, no matter whether the membrane was already permeabilized or not [8,9].

Moreover, with long enough interpulse intervals (e.g., 10–30 s), cells become more sensitive to new pulses, a phenomenon known as electrosensitization [10–13]. A pre-exposure to electroporation pulses, or conditioning, can enhance the effect of the next electroporation treatment as much as 2.5 times (25 °C) or even 6 times (37 °C) [10]. Such hypersensitivity results from biological rather than just physical-chemical effects of electroporation, although its exact mechanism remains elusive. Electrosensitization also explains higher efficiency of electric pulses delivered at low repetition rates, when the total treatment becomes lengthy enough to let sensitization develop. Alternatively, longer inter-pulse intervals could allow more time for membrane resealing, so the treatment as a whole becomes more effective [4,5]; the discrimination of this mechanism from the biological effect of sensitization may be difficult since both processes can develop concurrently.

Shortening the time interval between pulses to single microseconds and below should preclude any changes in cells’ susceptibility due to active biological responses. Therefore any observed changes could be attributed to physical-chemical effects, such as the formation of short-lived membrane pores. It has long been contemplated that electroporation produces two distinctly different types of pores, namely the short- and long-lived ones [9,14–17]. The short-lived pores are numerous but reseal within milliseconds and thereby contribute little to

the transmembrane transport (this concept, however, was recently challenged [18]). The formation and resealing of short-lived pores can be detected by the increased conductance of a dense cell suspension in 10 ms after an electroporating pulse, with almost complete restoration of conductance in 100 ms [9]. The long-lived pores, on the contrary, are too few to significantly increase the membrane conductance, but contribute more to the membrane transport due to their long lifespan, seconds to hours [8,9,17,19–21]. The fraction (number and/or size) of long-lived pores is at least an order of magnitude smaller than short-lived pores [9], so their impact on the membrane conductance is relatively small.

This model suggests that electroporation should be less efficient if a new pulse is applied when the short-lived pores are still open (e.g., within <10 ms after the previous pulse). However, Vernier et al. [22] reported the uptake of propidium and YP only when the interval between 4-ns pulses was reduced from 100 or 10 ms down to 1 or 0.1 ms, as if the cells became more vulnerable within the short time window after the previous pulse. Our recent study showed that a second 300-ns pulse, applied 50 μs after the first one, increases YP uptake twofold [23]. Reducing the inter-pulse interval from 100 ms to 1 ms (sixty 300-ns pulses), or even from 1 or 10 s down to 1 ms (two 9-μs pulses) did not change the survival of electroporated U937 and Jurkat cells [12]. Delivering 10, 600-ns pulses at various intervals from 200 ms down to 1.4 μs caused essentially the same propidium uptake in CHO cells [24], suggesting that the short lived-pores had no impact. The same study also reported that the effect of a train of ten 600-ns pulses delivered at 50, 250 or 500 kHz (i.e., with gaps of 19.4, 3.4, or 1.4 μs) caused less membrane disruption than a single pulse of the same intensity but 10-fold duration (6 μs). For two of the tested permeabilization markers (propidium and FM1–43 dye), the effect of a train of pulses with the shortest gap of 1.4 μs was as much as 50% smaller than after a single 6 μs pulse. A paradox presented by these data is that a single 6 μs pulse can be viewed as ten 600-ns pulses with zero gaps – hence the reduction of the gap from 1.4 μs further towards zero should at some point start producing stronger effects. The only alternative to this expectation would be a reduction of the effect by any transient turn off of the applied electric field, no matter how brief it is.

In fact, the latter idea bridges with a recently discovered phenomenon of bipolar cancellation [23,25–28]. Indeed, the reversal of the pulse polarity, or the delivery of a 2nd pulse of the opposite polarity shortly after the first one, profoundly reduces the efficiency of diverse electroporation treatments. Bipolar cancellation is limited to pulses of nanosecond duration (perhaps up to several μs) and the inter-pulse intervals of up to 10–50 μs. Bipolar cancellation takes place even if the 2nd phase (or the 2nd pulse of the opposite polarity) is reduced to 35% of the first phase [27] or to just 10–20% (unpublished data). Then, one may expect that a brief reduction of the applied field down to zero, even without inverting its polarity, might also have some “canceling effect”. The mechanism responsible for the bipolar cancellation has not been established, and the processes of membrane pore formation by nanosecond electric pulses (nsEP) and their elimination are far from being understood. This project aimed at getting a new insight into these processes by analyzing electropermeabilization of cells by closely spaced paired nsEP of the same polarity. We explored inter-pulse intervals shorter than in previous studies (down to 0.4 μs) and established only additive effects on YP uptake, as well as only additive and supra-additive effects on Tl^{+} entry and Ca^{2+} entry and mobilization; these findings further challenge the

concept that formation of short-lived pores reduces sensitivity to electroporation. We also revealed a previously unknown specific effect of closely spaced pulses on Ca^{2+} mobilization from ER.

2. Materials and methods

2.1. Cells and media

Chinese hamster ovary cells (CHO-K1) and a murine neuroblastoma-rat glioma hybrid (NG108) were purchased from the American Type Culture Collection (ATCC, Manassas, VA). CHO cells were propagated in Ham's F12 K medium (Mediatech Cellgro, Herdon, VA) supplemented with 10% fetal bovine serum (FBS). NG108 cells were grown in Dulbecco's Modified Eagle's medium (Caisson Labs, North Logan, UT) without sodium pyruvate, supplemented with 4 mM L-glutamine, 4.5 g/l glucose, 10% FBS, 0.2 mM hypoxanthine, 400 nM aminopterin, and 0.016 mM thymidine. Both cell lines were cultured at 37 °C with 5% CO_2 in air. 100 I.U./ml penicillin and 0.1 μg/ml streptomycin were added to culture media to prevent contamination. The media supplements were from Sigma-Aldrich (St. Louis, MO) except for the serum (Atlanta Biologicals, Norcross, GA). Cells were seeded onto "0" thickness glass coverslips 12–24 h before the experiments.

2.2. Calcium imaging, YO-PRO-1 and Tl^+ uptake measurements

The cytosolic free Ca^{2+} concentration ($[Ca^{2+}]_i$) was monitored by time lapse ratiometric fluorescence imaging with Fura-2. The detailed procedures can be found in our previous publications [29,30]. Briefly, cells on glass coverslips were loaded with 5 μM of Fura-2AM (Teflabs, Austin, TX) with 0.02% of Pluronic F-127 (Sigma-Aldrich) for 30 min at room temperature in the dark. The coverslips were transferred into a glass-bottomed chamber mounted on an IX71 microscope (Olympus America, Center Valley, PA) and rinsed for 15 min with a physiological solution containing (in mM): 140 NaCl, 5.4 KCl, 1.5 $MgCl_2$, 2 $CaCl_2$, 10 Glucose, and 10 HEPES (pH 7.3, 290–300 mOsm/kg). Afterwards, the solution was refreshed every 5 min using a VC-6 valve controller system (Warner Instruments, Hamden, CT).

Fura-2 was excited alternatively at 340 and 380 nm using a fast wavelength switcher Lambda DG4 (Sutter Instruments, Novato, CA). Fluorescence images at 510 nm were collected with a UApoN340 40×/1.35 objective (Olympus) and an iXon Ultra 897 back-illuminated CCD Camera (Andor Technology, Belfast, UK), and processed with Metafluor v. 7.5 software (Molecular Devices, Sunnyvale, CA). Time lapse recordings at a rate of 10 images/s started 30 s prior to nsEP application and continued for 5 min.

For experiments in Ca^{2+}-free medium, $CaCl_2$ was omitted, and the solution was passed through a column packed with Calcium Sponge S (Thermo Fisher Scientific, Waltham, MA) to remove residual Ca^{2+}. As measured with Fura-2 added to the physiological solution, the residual Ca^{2+} level after Calcium Sponge S treatment did not exceed 100 nM.

In order to isolate nsEP-induced Ca^{2+} influx through the cell membrane, the ER Ca^{2+} stores were depleted by perfusion with 20 μM cyclopiazonic acid (CPA) in the physiological solution. It caused Ca^{2+} leak from ER, seen as a transient increase in the cytosolic Ca^{2+}

level, followed by a gradual recovery to the initial level in 15–20 min. Cells with incomplete restoration of the initial Ca^{2+} level were not used for experiments.

To study YP uptake, 1 μM of the dye was added to the physiological solution. Lambda DG4 and FITC filter set (Chroma Technology, Bellows Falls, VT) were utilized to excite fluorescence of YP and to collect the emission of the dye. Recordings of YP uptake started 60 s prior to nsEP application and continued for 5 min after it, once in 20 s. YP fluorescence was corrected for the passive uptake of the dye, as measured in sham-exposed cells. Data were presented as $F\text{-}F_0$ where F_0 is YP fluorescence before nsEP exposure (the average of the first three datapoints).

To study Tl^+ uptake, CHO cells were loaded with a Tl^+-sensitive dye (Thallos™ No Wash Potassium Channel Assay Kit, Teflabs, Austin, TX) following the supplier's recommendations. Thallos™ fluorescent dye in DMSO with 7% of Pluronic F-127 and Probenecid were added to Hank's Balanced Salt Solution provided with the kit to make the loading buffer. CHO cells on coverslips were loaded for 30 min at room temperature in the dark, then transferred into the physiological solution in the perfusion chamber on microscope stage. Lambda DG4 and a FITC filter set were utilized to excite fluorescence and to collect emission of the dye. Before each recording, solution in the chamber was substituted for 20 s with a Tl^+-containing buffer composed of (in mM): 140 Sodium Acetate, 5.4 Potassium Acetate, 1.5 $MgSO_4$, 10 glucose, 10 HEPES, and 5 Tl_2SO_4 (pH 7.3). Images were taken at 10 frames/s for 10 s prior to nsEP and for 30 s after it while continuing superfusion with the Tl^+-containing buffer. The data for sham-exposed samples were subtracted to correct for passive Tl^+ uptake, and the subsequent analysis was the same as described above for YP uptake experiments. Each coverslip was used for only one experiment.

All chemicals were purchased from Sigma-Aldrich except for CPA purchased from Tocris Bioscience (Bristol, UK).

2.3. nsEP exposure

The pulsed power system consisted of two independent, identical nanosecond pulse generators. Each generator had a fully charged capacitor that was turned on and off by a power MOSFET switch (model IXFB38N100Q2, IXYS, Milpitas, CA) for given periods of time. As the two generators worked in parallel, they delivered two unipolar pulses to the electrodes. Each generator's output was equipped with a forward-biased diode to decouple the generators from interfering with each other. Charging voltages, turn-on times and pulse durations of each generator were controlled separately. Two DC power supplies and two trigger channels were employed to drive the whole pulsed power system. Overall, the flexibility of the system allowed for the delivery of a single or paired pulses with equal or different amplitudes. The interpulse interval (0.4, 1, 10, 100, 1000 μs) and pulse duration (300 and 600 ns) were varied using BNC Pulse Generator Model 577 (Berkeley Nucleonics, San Rafael, CA) (Fig. 1). Pulses were monitored using 4 GHz, 20 Gs/s TDS7404 oscilloscope (Tektronix, Beaverton, OR).

The method of electroporation of individual selected cells on a microscope stage was described in detail previously [29–31]. In brief, an MPC-200 robotic manipulator (Sutter Instruments) was employed to position a pair of tungsten electrodes (with diameter of 100 μm) precisely at 50 μm above the surface of the coverslip. The only cells exposed to nsEP were those between the tips of the electrodes (170 μm gap). The electric field at the location of the cells was determined by 3D simulations with the finite-element Maxwell equation solver COMSOL Multiphysics Release 5.0. (Stockholm, Sweden). 300- and 600-ns pulses at the electric field strength from 3.7 to 11.1 kV/cm were used in this study. The pulsed power system was triggered and synchronized with the image acquisition and the perfusion system by a TLL pulse protocol using a Digidata 1440A board and by the Clampex v. 10.2 software (Molecular Devices). In all experiments, each cell or group of cells was subjected to nsEP exposure only once.

3. Results

3.1. Additive effect of paired pulses and of increasing the pulse width on YP uptake

A single 300- or 600-ns pulse at 3.7 kV/cm, as well as paired 300-ns pulses at intervals from 0.4 to 1000 μs triggered immediate YP uptake in NG108 cells (Fig. 2A). The uptake continued while gradually slowing down during the next 5 min of observation. The fluorescence level reached by the end of observation was similar in cells subjected to a single 600-ns pulse and a pair of 300-ns pulses, regardless of the interpulse interval; this level was twofold larger than in cells exposed to a single 300-ns pulse (Fig. 2A, right panel). A 3-fold increase in the electric field strength did not change this additive fashion of YP uptake (Fig. 2B).

In CHO cells, a single 300-ns pulse at 3.7 kV/cm caused YP uptake too small for a quantitative analysis, hence we tested a higher field strength of 7.4 kV/cm. Fig. 2C shows the additive effect of paired pulses on YP uptake for all interpulse intervals, similarly to NG108 cells.

3.2. Paradoxical potentiation of Ca^{2+}-response by closest-spaced paired 300-ns pulses

In contrast to the predominantly passive process of YP uptake by electroporated cells, changes in the cytosolic Ca^{2+} level are monitored and actively controlled by biological mechanisms. Ca^{2+} entry through an electroporated plasma membrane or leak from electroporated ER stores may trigger a positive feedback mechanism of calcium-induced calcium release (CICR) which will further amplify large enough Ca^{2+} signals but smaller Ca^{2+} changes will be ignored as “noise” [29,30,32]. Concurrently, Ca^{2+} is actively removed from the cytosol by specific pumps and exchangers, returning its concentration to the pre-treatment level in about 5 min after 3.7–4.5 kV/cm stimuli (Fig. 3).

Notwithstanding the active control, Ca^{2+} transients evoked by a single 600-ns pulse in NG108 cells at 3.7 kV/cm were twice the amplitude of those elicited by a single 300-ns pulse (Fig. 3A, left panel). In CHO cells, the effect was strongly supra-additive (Fig. 3B & C), consistent with our previous studies which showed strong impact of CICR in these cells [29,30]. However, the additional increase of the transients elicited by closest-spaced paired

pulses (Fig. 3A and B, 0.4 and 1 μs), as compared to either one 600-ns pulse or paired pulses with longer intervals, was unexpected and difficult to explain by any known mechanisms. This paradoxical potentiation disappeared when the electric field was increased to 4.5 kV/cm, possibly because of the saturation of the CICR mechanism (Fig. 3C).

3.3. The closest-spaced paired 300-ns pulses specifically target Ca^{2+} release/efflux from the ER

As shown earlier, Ca^{2+} transients elicited by nsEP in CHO cells are formed by extracellular Ca^{2+} entry, as well as by passive efflux and active release from the ER, whereas mitochondrial Ca^{2+} played no role [29,30]. Therefore the following experiments were aimed at defining the role of extracellular Ca^{2+} and ER Ca^{2+} in the potentiation of the transients evoked by closest-spaced paired pulses. We checked if this potentiation is preserved or altered by depletion of the ER Ca^{2+} store (Fig. 4) and by removal of extracellular Ca^{2+} (Fig. 5).

The depletion of Ca^{2+} from ER was accomplished by perfusion of cells with 20 μM cyclopiazonic acid (CPA). It expectedly abolished the CICR mechanism and reduced the transients amplified by this mechanism, i.e., those evoked by both 600-ns pulses and paired 300-ns pulses. In contrast, it increased the response to a single 300-ns pulse (which was initially too small to trigger the release), probably by inhibiting pumps responsible for Ca^{2+} removal from the cytosol. The parallel control experiments showed strong potentiation of the response by paired pulses spaced at 0.4 μs (Fig. 4), which serves as an independent replication of the data presented in Fig. 3. Depletion of Ca^{2+} from the ER eliminated this potentiation, resulting in the responses to paired pulses at 0.4 μs interval and to a single 600-ns pulse becoming similar.

In order to produce measurable Ca^{2+} transients in a Ca^{2+}-free medium (i.e., due to solely Ca^{2+} efflux and active release from the ER), the electric field had to be increased to 11.1 kV/cm (Fig. 5). Nonetheless, the effects elicited by single pulses at both pulse widths, as well as by paired pulses at “longer” intervals of 100–1000 μs, measured just 20–50 nM and in all cells were too weak to elicit amplification by CICR; a comparison between these groups would be unreliable due to the small amplitude of the effect.

In contrast, closest-spaced paired pulses elicited the response large enough to trigger CICR in 21 out of 41 cells (0.4 μs interval) and in 6 out of 40 cells (1 μs interval). Such CICR-amplified transients are clearly distinguishable from non-amplified responses, and are shown separately in the respective panels in Fig. 5. The data averaged across all the cells (irrespective of CICR) also showed strong potentiation by the closest-spaced paired pulses (Fig. 5, right panel).

3.4. Lack of paired-pulse potentiation for Tl^{+} entry through permeabilized plasma membrane

Fluorescence detection of Tl^{+} uptake is a powerful approach to detect cell membrane electroporation; it is more sensitive than YP uptake detection [33], despite the possibility of concurrent Tl^{+} entry through some endogenous cation channels. Compared to the generation

of Ca^{2+} transients, Tl^{+} entry is a much simpler process as there are no intracellular Tl^{+} stores, amplification by a CICR-like mechanism, or active extrusion from the cytosol.

The pattern of Tl^{+} uptake following electropermeabilization (Fig. 6) was similar to YP uptake (Fig. 2), with the exception of supra-additive effect for a single 600-ns pulse and paired pulses with 0.4 μs interval, as compared to a single 300-ns stimulus. However, there was no additional potentiation of the response by the closely-spaced pulses compared to a single 600-ns pulse. This lack of supra-additivity contrasts Ca^{2+} mobilization data and thereby emphasizes the contribution of intracellular reservoirs to Ca^{2+} response.

4. Discussion

In this work, we evaluated the effects of paired 300-ns pulses at intervals shorter than previously tested. We consistently observed three different types of effects:

1. Simple additive effects for the uptake of YP dye. In two different cell types, for the electric field intensity from 3.7 to 11.1 kV/cm, and for inter-pulse intervals from 0.4 to 1000 μs, the effect of two 300-ns pulses was twofold larger than the effect of a single pulse, and it was the same as the effect of a single pulse of double duration (600 ns). These data complement our earlier findings of the additive uptake of YP for paired pulses at 50 μs intervals in both regular and low-conductance solutions [23], and for multiple pulses applied with 1-s intervals [8]. In other words, the first 300-ns pulse did not change the electroporation efficiency of the second pulse, and each pulse opened the same number of long-lived YP-permeable pores (see [8] for discussion why it was the pore number rather than pore size). These data provided no evidence for the existence of short-lived pores after a 300-ns pulse; or the efficiency of the second pulse somehow did not depend on the presence of short-lived pores. We did not observe a biphasic dependence of YP uptake on the pulse repetition rate [24], with deviations of about 20% from the average value. It is, however, possible that the delivery of 10 pulses in this study might emphasize the minor fluctuations which we saw with paired pulses (Fig. 2, right column), and the non-significant dip seen at 10 μs interval could develop into the reported minimum of YP at 50 kHz (20 μs interval).

2. Supra-additive effect for the closest-spaced paired pulses (0.4 and 1 μs), as well as for a double-duration single pulse. This pattern of response was typical for Ca^{2+} transients elicited after depletion of intracellular Ca^{2+} stores (Fig. 4), for Ca^{2+} transients evoked by high-amplitude pulses (possibly because of saturation of CICR mechanism, so it contributed similarly to all stimuli, Fig. 3C), and for Tl^{+} uptake (Fig. 5). As with the YP uptake data, these results provided no support to possible impact of short-lived pores on the efficiency of the second electroporating pulse. Moreover, the data suggest that the first pulse may produce some “latent pores” or “pre-pores” [34], so the second pulse not only opens the new pores, but also converts the latent pores into active ones. The fact that we did not observe this supra-additive pattern for YP uptake may indicate that it

involves endogenous cation channels (permeable to Ca^{2+} and Tl^{+} but not to YP) which get damaged or modified by the electric field pulses.

3. Additional supra-additive effect for the closest-spaced paired pulses (0.4 and 1 μs), when they caused significantly larger response than a single double-duration pulse (Fig. 3, A, B, and Fig. 5). This paradoxical type of response was observed only for Ca^{2+} transients which involved CICR and/or passive Ca^{2+} efflux from the ER. We do not know if the increased Ca^{2+} efflux elicited CICR, or the paired pulses somehow facilitated CICR mechanism. Future studies may separate between these two mechanisms by testing if the supra-additive response is preserved after pharmacological inhibition of CICR [29,30]. Either way, we conclude that the closest-spaced paired pulses specifically target ER Ca^{2+} stores, by a mechanism that has yet to be established. One may hypothesize that permeabilization of the plasma membrane by the first pulse makes the ER more vulnerable to the second one; it can be validated by testing for the supra-additive response in the presence of electroporation inhibitor Gd^{3+} [35,36]. The ability to target ER may be particularly important for medical applications in tissues that rely heavily on CICR, such as muscle and cardiac stimulation [37].

Our data did not support the idea set forth in the Introduction, that the removal of the applied field may cause cancellation even without the electric field reversal. We have not observed it for any of the studied endpoints and therefore conclude that the field reversal is essential for bipolar cancellation to occur. We also conclude that, for studies of bipolar cancellation, the effects of two opposite-polarity pulses should be compared to the effect of two same polarity pulses, rather than to a single unipolar pulse.

Our results, regardless of the protocol and permeabilization marker tested, provided no indication of the formation of short-lived pores after a single 300-ns pulse. One can speculate that the pulses were intense enough to open the long-lived pores but not the short-lived ones; however, this would contradict the current view that the former evolve from the latter. Instead, this would mean that the two types of pores are indeed different, e.g., one of them involves membrane proteins while the other one is purely lipidic. It may also be a specific feature of nsEP that either they are less efficient in creating short-lived pores than the conventional (“long”) electroporation pulses, or they permeabilize cell membrane regardless of the presence of short-lived pores. Future work in this direction may substantially change our understanding and existing concepts of the electroporation process.

Acknowledgments

The study was supported by an AFOSR MURI grant FA9550-15-1-0517 (to AGP) on Nanoelectropulse-Induced Electromechanical Signaling and Control of Biological Systems, administered through Old Dominion University, AFOSR-LRIR 16RHCOR348 (to BLI), and by R01HL128381 from NHLBI (to AGP).

References

1. Neumann, E., Sowers, AE., Jordan, CA. Electroporation and Electrofusion in Cell Biology. Plenum; New York: 1989.
2. Zimmermann, U., Neil, GA. Electromanipulation of Cells. CRC Press; Boca Raton: 1996.

3. Pakhomov, AG., Miklavcic, D., Markov, MS. Advanced Electroporation Techniques in Biology in Medicine. CRC Press; Boca Raton: 2010. p. 528
4. Silve A, Guimera Brunet A, Al-Sakere B, Ivorra A, Mir LM. Comparison of the effects of the repetition rate between microsecond and nanosecond pulses: electropermeabilization-induced electro-desensitization? Biochim Biophys Acta. 2014; 1840:2139–2151. [PubMed: 24589913]
5. Lamberti P, Romeo S, Sannino A, Zeni L, Zeni O. The role of pulse repetition rate in nsPEF-induced electroporation: a biological and numerical investigation. IEEE Trans Biomed Eng. 2015; 62:2234–2243. [PubMed: 25850084]
6. Kotnik T, Macek-Lebar A, Miklavcic D, Mir LM. Evaluation of cell membrane electropermeabilization by means of a nonpermeant cytotoxic agent. BioTechniques. 2000; 28:921–926. [PubMed: 10818698]
7. Rols MP, Teissie J. Electropermeabilization of mammalian cells. Quantitative analysis of the phenomenon. Biophys J. 1990; 58:1089–1098. [PubMed: 2291935]
8. Pakhomov AG, Gianulis E, Vernier PT, Semenov I, Xiao S, Pakhomova ON. Multiple nanosecond electric pulses increase the number but not the size of long-lived nanopores in the cell membrane. Biochim Biophys Acta. 2015; 1848:958–966. [PubMed: 25585279]
9. Pavlin M, Miklavcic D. Theoretical and experimental analysis of conductivity, ion diffusion and molecular transport during cell electroporation—relation between short-lived and long-lived pores. Bioelectrochemistry. 2008; 74:38–46. [PubMed: 18499534]
10. Jensen SD, Khorokhorina VA, Muratori C, Pakhomov AG, Pakhomova ON. Delayed hypersensitivity to nanosecond pulsed electric field in electroporated cells. Sci Rep. 2017; 7:10992. [PubMed: 28887559]
11. Pakhomova ON, Gregory BW, Pakhomov AG. Facilitation of electroporative drug uptake and cell killing by electrosensitization. J Cell Mol Med. 2013; 17:154–159. [PubMed: 23305510]
12. Pakhomova ON, Gregory BW, Khorokhorina VA, Bowman AM, Xiao S, Pakhomov AG. Electroporation-induced electrosensitization. PLoS One. 2011; 6:e17100. [PubMed: 21347394]
13. Dermol J, Pakhomova ON, Pakhomov AG, Miklavcic D. Cell Electrosensitization exists only in certain electroporation buffers. PLoS One. 2016; 11:e0159434. [PubMed: 27454174]
14. Teissie J, Golzio M, Rols MP. Mechanisms of cell membrane electropermeabilization: a minireview of our present (lack of ?) knowledge. Biochim Biophys Acta. 2005; 1724:270–280. [PubMed: 15951114]
15. Weaver JC, Chizmadzhev YA. Theory of electroporation: a review. Bioelectrochem Bioenerg. 1996; 41:135–160.
16. Saulis G, Venslauskas MS, Naktinis J. Kinetics of pore resealing in cell membranes after electroporation. Bioelectrochem Bioenerg. 1991; 26:1–13.
17. Saulis G. Kinetics of pore disappearance in a cell after electroporation. Biomed Sci Instrum. 1999; 35:409–414. [PubMed: 11143387]
18. Schoenbach KH, Pakhomov AG, Semenov I, Xiao S, Pakhomova ON, Ibey BL. Ion transport into cells exposed to monopolar and bipolar nanosecond pulses. Bioelectrochemistry. 2015; 103:44–51. [PubMed: 25212701]
19. Kinosita K Jr, Tsong TY. Formation and resealing of pores of controlled sizes in human erythrocyte membrane. Nature. 1977; 268:438–441. [PubMed: 895849]
20. Pakhomova ON, Gregory B, Semenov I, Pakhomov AG. Calcium-mediated pore expansion and cell death following nanoelectroporation. Biochim Biophys Acta. 2014; 1838:2547–2554. [PubMed: 24978108]
21. Pakhomov AG, Bowman AM, Ibey BL, Andre FM, Pakhomova ON, Schoenbach KH. Lipid nanopores can form a stable, ion channel-like conduction pathway in cell membrane. Biochem Biophys Res Commun. 2009; 385:181–186. [PubMed: 19450553]
22. Vernier PT, Sun Y, Gundersen MA. Nanoelectropulse-driven membrane perturbation and small molecule permeabilization. BMC Cell Biol. 2006; 7:37. [PubMed: 17052354]
23. Gianulis EC, Casciola M, Xiao S, Pakhomova ON, Pakhomov AG. Electropermeabilization by uni- or bipolar nanosecond electric pulses: the impact of extracellular conductivity. Bioelectrochemistry. 2017; 119:10–19. [PubMed: 28865240]

24. Steelman ZA, Tolstykh GP, Beier HT, Ibey BL. Cellular response to high pulse repetition rate nanosecond pulses varies with fluorescent marker identity. Biochem Biophys Res Commun. 2016; 478:1261–1267. [PubMed: 27553279]
25. Ibey BL, Ullery JC, Pakhomova ON, Roth CC, Semenov I, Beier HT, Tarango M, Xiao S, Schoenbach KH, Pakhomov AG. Bipolar nanosecond electric pulses are less efficient at electropermeabilization and killing cells than monopolar pulses. Biochem Biophys Res Commun. 2014; 443:568–573. [PubMed: 24332942]
26. Pakhomov AG, Semenov I, Xiao S, Pakhomova ON, Gregory B, Schoenbach KH, Ullery JC, Beier HT, Rajulapati SR, Ibey BL. Cancellation of cellular responses to nanoelectroporation by reversing the stimulus polarity. Cell Mol Life Sci. 2014; 71:4431–4441. [PubMed: 24748074]
27. Gianulis EC, Lee J, Jiang C, Xiao S, Ibey BL, Pakhomov AG. Electroporation of mammalian cells by nanosecond electric field oscillations and its inhibition by the electric field reversal. Sci Rep. 2015; 5:13818. [PubMed: 26348662]
28. Merla C, Pakhomov AG, Semenov I, Vernier PT. Frequency spectrum of induced transmembrane potential and permeabilization efficacy of bipolar electric pulses. Biochim Biophys Acta. 2017; 1859:1282–1290. [PubMed: 28432034]
29. Semenov I, Xiao S, Pakhomova ON, Pakhomov AG. Recruitment of the intracellular Ca2+ by ultrashort electric stimuli: the impact of pulse duration. Cell Calcium. 2013; 54:145–150. [PubMed: 23777980]
30. Semenov I, Xiao S, Pakhomov AG. Primary pathways of intracellular Ca(2+) mobilization by nanosecond pulsed electric field. Biochim Biophys Acta. 2013; 1828:981–989. [PubMed: 23220180]
31. Pakhomov AG, Semenov I, Casciola M, Xiao S. Neuronal excitation and permeabilization by 200-ns pulsed electric field: an optical membrane potential study with FluoVolt dye. Biochim Biophys Acta. 2017; 1859:1273–1281. [PubMed: 28432032]
32. Putney JW Jr, Ribeiro CM. Signaling pathways between the plasma membrane and endoplasmic reticulum calcium stores. Cell Mol Life Sci. 2000; 57:1272–1286. [PubMed: 11028918]
33. Bowman AM, Nesin OM, Pakhomova ON, Pakhomov AG. Analysis of plasma membrane integrity by fluorescent detection of Tl(+) uptake. J Membr Biol. 2010; 236:15–26. [PubMed: 20623351]
34. Melikov KC, Frolov VA, Shcherbakov A, Samsonov AV, Chizmadzhev YA, Chernomordik LV. Voltage-induced nonconductive pre-pores and metastable single pores in unmodified planar lipid bilayer. Biophys J. 2001; 80:1829–1836. [PubMed: 11259296]
35. Gianulis EC, Pakhomov AG. Gadolinium modifies the cell membrane to inhibit permeabilization by nanosecond electric pulses. Arch Biochem Biophys. 2015; 570:1–7. [PubMed: 25707556]
36. Andre FM, Rassokhin MA, Bowman AM, Pakhomov AG. Gadolinium blocks membrane permeabilization induced by nanosecond electric pulses and reduces cell death. Bioelectrochemistry. 2010; 79:95–100. [PubMed: 20097138]
37. Eisner DA, Caldwell JL, Kistamas K, Trafford AW. Calcium and excitation-contraction coupling in the heart. Circ Res. 2017; 121:181–195. [PubMed: 28684623]

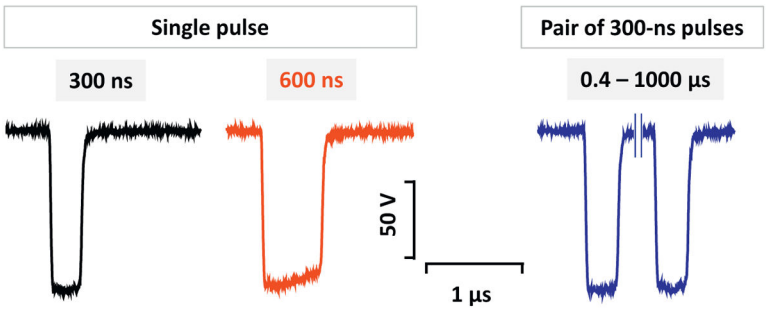

Fig. 1.

Representative traces of a 300- and a 600-ns pulse, and of a pair of 300-ns pulses.

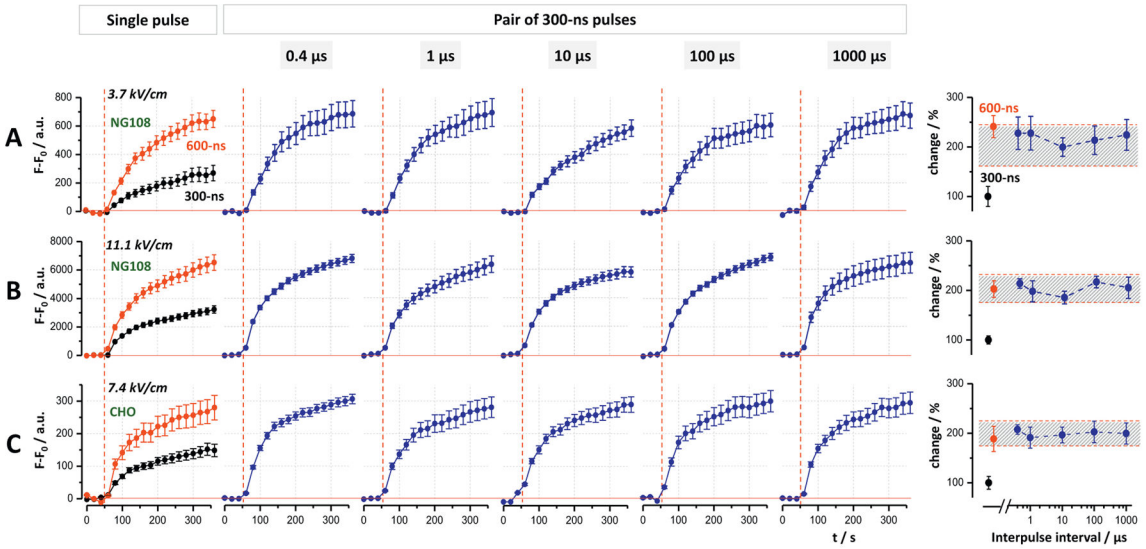

Fig. 2.

Single 600-ns pulses and paired 300-ns pulses at all interpulse intervals cause twice more YO-PRO-1 uptake than a single 300-ns pulse. The experiments were performed in NG108 cells (A and B) and CHO cells (C). The field strength was 3.7 kV/cm (A), 11.1 kV/cm (B), and 7.4 kV/cm (C). Individual panels show YO-PRO-1 uptake over time induced by single 300- and 600-ns pulses (left column) and by paired 300-ns pulses at the indicated interpulse intervals. Vertical dashed lines show when nsEP was applied. Graphs at the right show the final dye uptake values plotted against the interpulse interval; the response to a single 300-ns pulse was taken as 100%. The shaded area is centered at the 200% effect, with limits twice the error bars for a single pulse. Mean ± s.e. for $n \geq 60$.

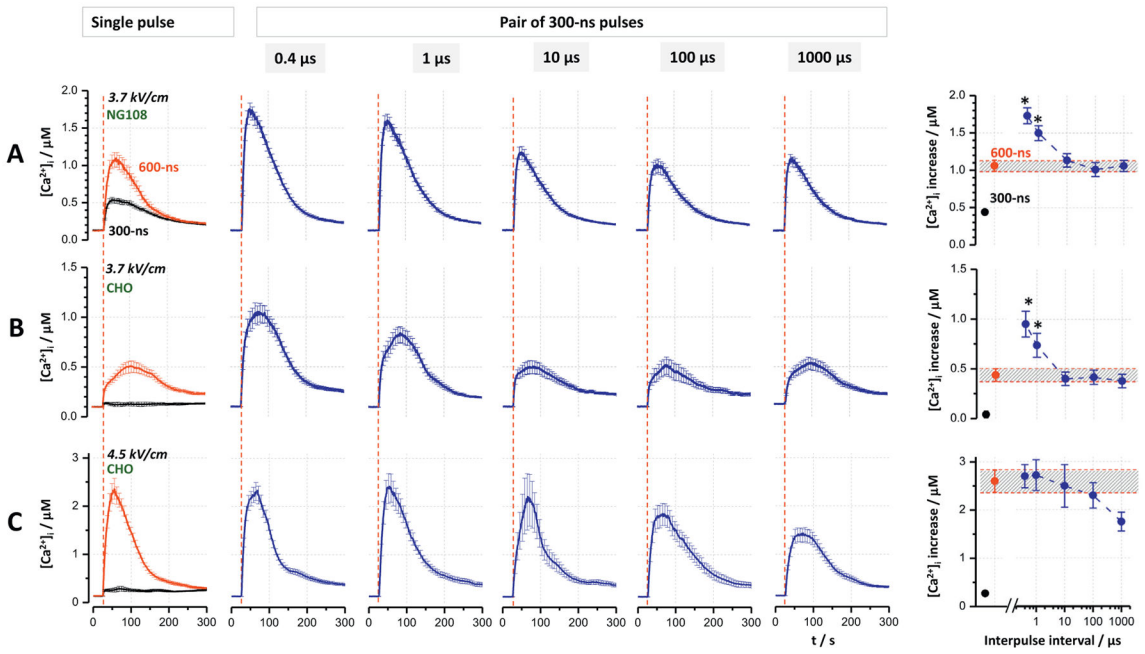

Fig. 3.

Paired 300-ns pulses at the shortest interpulse intervals can cause larger $[Ca^{2+}]_i$ increase than a single 600-ns pulse. The experiments were performed in NG108 (A) and CHO cells (B and C). The field strength was 3.7 kV/cm (A and B) and 4.5 kV/cm (C). Individual panels show Ca^{2+} transients induced by single 300- and 600-ns pulses (left column) and by paired 300-ns pulses at the indicated interpulse intervals. Vertical dashed lines show when nsEP was applied. Graphs at the right display the peak amplitude of Ca^{2+} transient against the interpulse interval. For easier comparison, the peak amplitude of the transients evoked by a single 600-ns pulse is emphasized by shading. The asterisks show significantly higher effect of paired 300-ns pulses compared to a single 600-ns pulse ($p < 0.05$, one-tailed *t*-test). Mean ± s.e. for n ≥ 60.

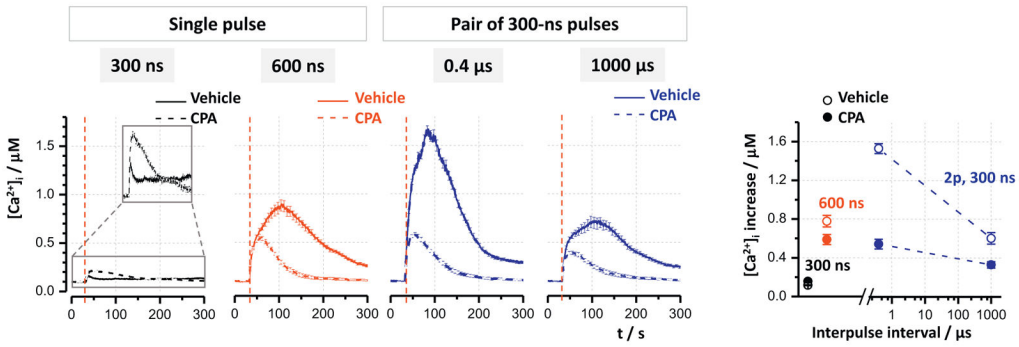

Fig. 4.

Depletion of Ca^{2+} from the endoplasmic reticulum eliminates the additional potentiation of Ca^{2+} transients by the closest-space paired pulses. CHO cells were exposed to 3.7 kV/cm pulses (vertical dashed lines) in the presence of 20 µM CPA (dashed lines) or vehicle (solid lines). The other nsEP parameters are indicated in the graphs. For clarity, small transients evoked by a single 300-ns pulse are shown magnified in the inset in the left panel. The graph at the right shows peak amplitudes of Ca^{2+} transients for the indicated conditions. Mean ± s.e. for $n \geq 30$.

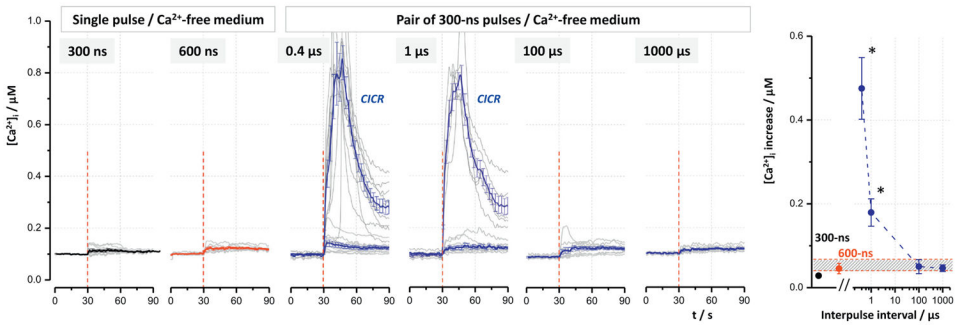

Fig. 5.

Facilitation of CICR by closest-spaced paired 300-ns pulses in the absence of extracellular Ca^{2+}. CHO cells were exposed to 11.1 kV/cm pulses at 30 s (vertical dashed line) in a Ca^{2+}-free medium. Individual panels show characteristic Ca^{2+} transients in individual cells (gray) and transients averaged for all cells (thicker lines with error bars, colored or black). nsEP exposure conditions are indicated in the graphs. Responses to a single pulse of either duration and to paired pulses with either 100 or 1000 µs gap were only 20–50 nM and never triggered CICR. In contrast, the closest-spaced paired pulses (0.4 and 1 µs intervals) activated CICR in 21 out of 41 cells and in 6 out of 40 cells, respectively. CIRC-amplified traces were averaged separately from the non-amplified ones. The right panel shows peak amplitudes of Ca^{2+} response averaged across all cells (CIRC-amplified and non-amplified pooled together) against the interpulse interval. See text and Fig. 3 for more details. Mean ± s.e., $n \geq 20$.

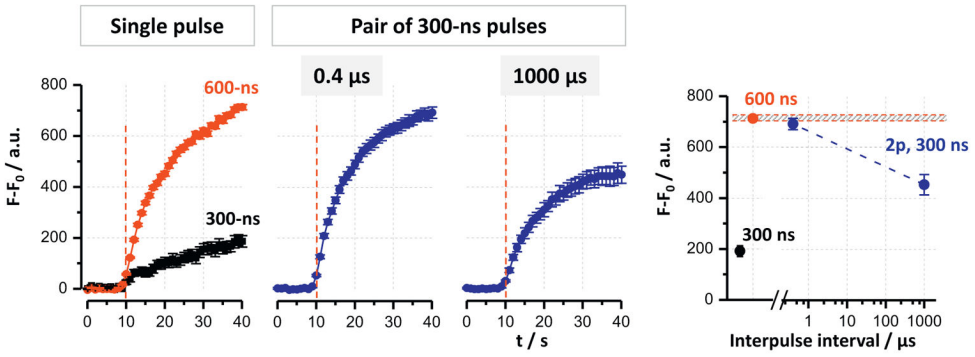

Fig. 6.

Tl^+ uptake is facilitated equally by doubling the pulse width and by applying paired 300-ns pulses at 0.4 µs interval. Individual panels show Tl^+ fluorescence over time in CHO cells subjected to 3.7 kV/cm nsEP. The right panel shows maximum fluorescence values by the end of recording (30 s after nsEP) for the indicated exposure conditions. See text and Fig. 3 for more details. Mean ± s.e. for $n \geq 40$.